Nonlinear vibration energy harvesting based on variable double well potential function

Wei Yang, Shahrzad Towfighian
State University of New York at Binghamton, Binghamton, NY, 13905
wyang24@binghamton.edu, stowfigh@binghamton.edu

ABSTRACT

Converting ambient mechanical energy to electricity, vibration energy harvesting, enables powering of the low-power remote sensors. Nonlinear energy harvesters have the advantage of a wider frequency spectrum compared to linear resonators making them more efficient in scavenging the broadband frequency of ambient vibrations. To increase the output power of the nonlinear resonators, we propose an energy harvester composed of a cantilever piezoelectric beam carrying a movable magnet facing a fixed magnet at a distance. The movable magnet on the beam is attached to a spring at the base of the beam. The spring-magnet system on the cantilever beam creates the variable double well potential function. The spring attached to the magnet is in its compressed position when the beam is not deflected, as the beam oscillates, the spring energy gradually releases and further increases the amplitude of vibration. To describe the motion of the cantilever beam, we obtained two coupled partial differential equations by assuming the cantilever beam as Euler-Bernoulli beam considering the effect of the moving magnet. Method of multiple scales is used to solve the coupled equations. The cantilever beam with the two magnets is a bi-stable system. Making one magnet movable can create internal resonance that is explored as a mechanism to increase the frequency bandwidth. The effect of system parameters on the frequency bandwidth of the resonator is investigated through numerical solutions. This study benefits vibration energy harvesting to achieve a higher performance when excited by the wideband ambient vibrations.

Keywords: Nonlinear energy harvesting, vibration, magnets, variable double well potential function, internal resonance

INTRODUCTION

Mechanical Vibration is one of the prevalent sources of ambient energy that can be converted to useful electrical energy for powering remote sensors. This renewable source of energy can eliminate changing of batteries, which is cumbersome and costly. Currently, most vibration based energy harvesters are designed as a linear resonator to achieve optimal performance by matching their natural frequency with the dominant ambient excitation frequencies. However in majority of cases, the ambient vibrations have a wide frequency spectrum at the low frequency range [1].

Several methods have been explored to solve the frequency bandwidth problem. A resonance frequency tunable energy harvester based on a magnetic force technique and a variable stiffness system has been studied [2]. Recently, to avoid frequency tuning after the initial set up of the harvester, exploiting the nonlinearities has become a solution for broadband energy harvesting. Researchers studied nonlinear oscillators with frequency hardening or softening [3-8] to broaden the frequency bandwidth. Stanton et al. [9] investigated the response of a bi-stable resonator with magnets to harmonic base excitation. Considering the actual ambient vibration, Ferrari [10], Daqaq [11] and Ando [12] analyzed the advantage of bi-stable system under random vibration input.

The contribution of this paper is to combine bi-stability and internal resonance effects to significantly broaden the frequency bandwidth. Bi-stability can broaden the frequency bandwidth, but the increase is not substantial. While bi-stability tilts the resonant peak to either direction, internal resonance causes the resonant peak to become two tilted branches facing opposite directions [13, 14]. This effect results in a larger frequency bandwidth that can increase energy conversion efficiency in vibration energy harvesting. The content of this article is organized as follows. In the next

Active and Passive Smart Structures and Integrated Systems 2016, edited by Gyuhae Park, Proc. of SPIE
Vol. 9799, 979902 · © 2016 SPIE · CCC code: 0277-786X/16/$18 · doi: 10.1117/12.2218077

section, the concept of variable double well potential is introduced. Then, a mathematical modelling of the combined resonator is presented followed by the perturbation method of multiple scales to solve for the steady-state frequency response. Numerical solutions are obtained next that show a double-jumping phenomenon.

1 VARIABLE DOUBLE WELL POTENTIAL FUNCTION CONCEPT

The system structure consists of a cantilever with movable spring-magnet and another fixed magnet as shown in Figure 1. The spring on the beam allows the movable magnet to move horizontally along the beam. The base of the beam and the base of the fixed magnet is on the shaker where it experiences ambient mechanical vibrations. The goal is to maximize the beam tip deflection, which is converted to electricity at the piezoelectric strip located at the beam base.

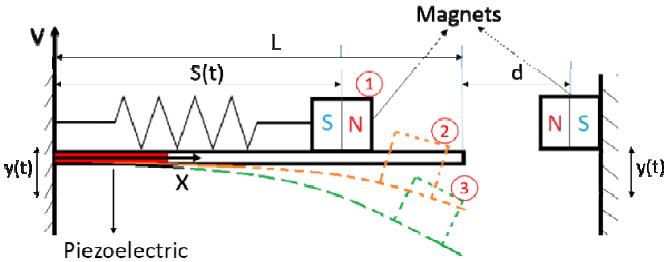

Figure 1 Schematic of a beam with movable magnet.

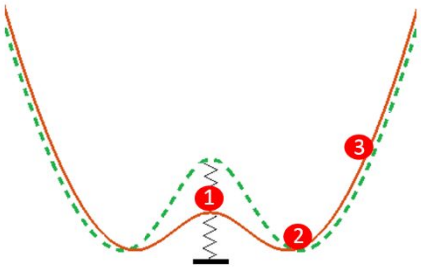

Figure 2 variable double well potential function concept

At the un-deflected beam position, the spring is fully compressed due to the magnetic repulsive force. As the beam vibrates and goes to the largest distance in vertical direction, the repulsive force decreases and the spring force dominates. Therefore it pushes the magnets to the tip of the cantilever. As the magnet tip gets closer to the fixed magnet, the oscillation amplitude can be increased even further from the repulsive force until it reaches a point where it does not go any further. Then it comes down gradually compressing the spring again as it approaches the zero position and the cycle repeats in the other direction.

Taking into account the presence of the repulsive magnetic force, the potential energy is a double well potential function for the magnetic distance below a certain threshold distance between two magnets (Figure 2). The role of the spring is to make a variable double well potential function. This can be described by the motion of a ball in a double well potential function with a flexible bump standing on a spring in the middle. The beam starts at the un-deflected position in the middle and goes down to the right stable point equivalent to the motion of the ball from point 1 to point 2 in the potential energy function. When the ball travels down, the spring releases and move the local maximum of the potential function up to form a new potential well that causes the ball to gain the stored energy of the spring. This energy helps the ball to have a higher initial velocity as it reaches point 2 leading to a larger height (point 3) compared to its original potential function. Reaching to point 3, where the velocity becomes zero and changes direction, the ball returns to position 2 and while traveling to the left, it compresses the spring gradually until its fully compressed position at point 1. Employing this variable potential function technique, the energy barrier is increased when the ball travels from point 1 to point 2 that increases the kinetic energy leading to a relatively higher travel position. The energy barrier is then decreased when the ball returns from point 2 to point 1 that saves the energy for the ball traveling in the opposite direction. The overall effect is that we take advantage of a lower energy barrier for increasing the range of oscillations of the beam resonator.

2 MATHEMATICAL MODELLING

To predict the dynamic response of the resonator, a mathematical model for the continuous model of the beam under the influence of magnets and the spring is derived. Our model is an extension of the model introduced by Siddiqui et al. [15] by adding the magnetic forces and base excitation. Various parameters used in the modelling are as follows. The beam

has the length L, area of cross-section A, volume density ρ, moment of inertia I and the modulus of elasticity E. The moving magnet slides along the length of the beam attached to a spring of stiffness k. The vertical deflection of the beam is given by v measured from the undeflected position of the beam and the position of the mass by s measured along the arc length of the beam, and F_{magx} and F_{magy} are the magnetic force in horizontal and vertical directions, respectively. N is the magnetization moment of magnet, μ_0 is the permeability of space, d is the distance between the tip of cantilever and fixed magnet, and y is the base excitation. The following normalized parameters are used.

$$\hat{s} = \frac{s}{L}\ ,\hat{v} = \frac{v}{L},\hat{x} = \frac{x}{L}, \hat{y} = \frac{y}{L}\ \ \hat{A} = \frac{A}{L^2}, \hat{m} = \frac{M}{\rho AL}\ ,\hat{t} = \frac{t}{\sqrt{\frac{\rho AL^4}{EI}}},\quad \omega_s = \sqrt{\frac{k\rho AL^4}{MEI}},\quad \hat{d} = \frac{d}{L},$$

$$\hat{D} = \frac{D}{L} = 1 + \hat{d} - \hat{s}\ ,\ \ \widehat{FR} = \frac{3\mu_0 N^2}{2\pi EIL^2}$$

For convenience the $\widehat{\ }$s are dropped. Using Hamilton method, the governing equations of motion are obtained

$$\ddot{s} + \omega_s^2 s + \ddot{v}v_x + v_x\ddot{y} + F_{magx}/m = 0 \tag{1}$$

$$\int_0^1 (v_{xxxx} + \ddot{v})dx + mf + \int_0^1 dx\ddot{y} + m\ddot{y} + F_{magy} = 0 \tag{2}$$

where the coupled acceleration term for the mass is

$$f = \ddot{v} + 2\dot{v_x}\dot{s} + v_{xx}\dot{s}^2 + v_x\ddot{s}$$

The first term in the above equation is the vertical acceleration of the beam, the second term is the Coriolis acceleration, the third is centripetal acceleration and the fourth term is the acceleration of the mass projected in the vertical direction. It should be noted that the above equations are written for small oscillations of the beam and is not valid for large oscillations.

$$F_{magx} = -FR(\frac{1}{D^4} - \frac{5v^2}{2D^6})$$

$$F_{magy} = FR(\frac{v}{D^5} - \frac{5v^3}{2D^7})$$

$$x = s$$

$$D = 1 + d - s$$

Using Rayleigh-Ritz method to reduce equation (1) and (2), we write variation formulations as

$$P(x) = \sum_{j=1}^{n} p_j\phi_j(x)$$

$$v(x,t) = \sum_{i=1}^{n} \alpha_i(t)\phi_i(x)$$

where $\phi_i(x)$ is the mode shape of cantilever, p_j is weighting function, α_j is unknown time varying coefficient and n is the number of mode shapes. Multiplying Equations (1) and (2) by $P(x)$, applying variation formulations, performing integration by parts and incorporating the boundary condition yields

$$\ddot{s} + \omega_s^2 s + \sum_{i=1}^{n} \ddot{\alpha_i}\phi_i \sum_{j=1}^{n} \alpha_j\phi_j' + \sum_{j=1}^{n} \alpha_j\phi_j'\ddot{y} - \frac{FR}{m}\left(\frac{1}{D^4} - \frac{5(\sum_{i=1}^{n} \alpha_i\phi_i)^2}{2D^6}\right) = 0 \tag{3}$$

$$\int_0^1 (\sum_{i=1}^n \alpha_i \phi_i'' \sum_{j=1}^n p_j \phi_j'' + \sum_{i=1}^n \ddot{\alpha_\iota} \phi_i \sum_{j=1}^n p_j \phi_j) dx + m \sum_{i=1}^n \ddot{\alpha_\iota} \phi_i \sum_{j=1}^n p_j \phi_j + m\ddot{s} \sum_{i=1}^n \alpha_i \phi_i' \sum_{j=1}^n p_j \phi_j +$$
$$m\dot{s}^2 \sum_{i=1}^n \alpha_i \phi_i'' \sum_{j=1}^n p_j \phi_j + 2m\dot{s} \sum_{i=1}^n \dot{\alpha_i} \phi_i' \sum_{j=1}^n p_j \phi_j + \sum_{j=1}^n p_j \phi_j \left(\int_0^1 dx + m \right) \ddot{y} + FR \left(\frac{\sum_{i=1}^n \alpha_i \phi_i}{D^5} - \frac{5(\sum_{i=1}^n \alpha_i \phi_i)^3}{2D^7} \right) = 0 \quad (4)$$

where P_i at $j = i$ is set to one and at other value $j \neq i$, is set to zero. The cantilever beam mode shapes for normalized parameters are given by:

$$\phi_i(x) = \cosh(k_i x) - \cos(k_i x) - \frac{\cos(k_i) + \cosh(k_i)}{\sin(k_i) + \sinh(k_i)} (\sinh(k_i x) - \sin(k_i x))$$

The static equilibrium equation is given by assuming $\alpha_i = 0$:

$$\omega_s^2 (s_0 - s_e) - \frac{FR}{m} \left(\frac{1}{D^4} \right) = 0$$

where s_0 is the original length of the spring, and s_e is the equilibrium position of moving magnet.

Dynamic equations of (3) and (4) are simplified using one mode shape. In order to obtain a solution, perturbation method of multiple scales is used. To further simplify the equations, the two equations are expanded about their equilibrium points (s_e for the moving magnet and $\alpha_i = 0$ for the beam). Taylor series up the second derivatives are used for the expansion and nonlinear terms higher than quadratic are dropped. Adding damping results in

$$\ddot{s} + \omega^2 s + 2\mu_1 \dot{s} + c_1 \ddot{\alpha_1} \alpha_1 + c_3 \alpha_1^2 + \alpha_1 \phi_1' \ddot{y} = 0 \quad (5)$$

$$\ddot{\alpha_1} + \omega_1^2 \alpha_1 + 2\mu_2 \dot{\alpha_1} + 2mc_7 s\ddot{\alpha_1} + 2mc_7 \dot{s}\dot{\alpha_1} + mc_7 \ddot{s}\alpha_1 + c_8 s\alpha_1 + (\phi_1 + s\phi_1')c_y \ddot{y} = 0 \quad (6)$$

where

$$\omega^2 = \omega_s^2 + c_2$$

$$c_1 = \phi_1 \phi_1'$$

$$c_2 = -\frac{FR}{m} \frac{4}{D^5}$$

$$c_3 = -\frac{FR}{m} \frac{a_2 \phi_1^2}{D^6}$$

$$\omega_1^2 = \frac{\int_0^1 \phi_1''^2 dx}{\int_0^1 \phi_1^2 dx + m\phi_1^2} + \frac{FR}{\int_0^1 \phi_1^2 dx + m\phi_1^2} \cdot \frac{\phi_1^2}{D^5}$$

$$c_7 = \frac{\phi_1 \phi_1'}{\int_0^1 1\phi_1^2 dx + m\phi_1^2}$$

$$c_8 = \frac{FR}{\int_0^1 \phi_1^2 dx + m\phi_1^2} \left(\frac{2\phi_1 \phi_1'}{D^5} + \frac{5\phi_1^2}{D^6} \right)$$

$$c_y = \frac{(\int_0^1 dx + m)}{\int_0^1 \phi_1^2 dx + m\phi_1^2}$$

$$D = 1 + d - s_e$$

3 PERTURBATION METHOD OF MULTIPLE SCALES

Method of multiple scales is used to study the qualitative behavior of the system under various parameters. The governing equations of (5) and (6) show that the system has parametric excitation. However, parametric counterpart has a zero steady-state response below the initiation threshold amplitude. This initiation threshold depends on the damping and level of excitation. In practice, the ambient vibration available is usually smaller than the threshold required to initiate the parametric excitation [16, 17]. Therefore, we do not consider parametric excitation in our case. Considering only the direct excitation, the two governing equations (5) and (6) become

$$\ddot{s} + \omega^2 s + 2\mu_1 \dot{s} + c_1 \ddot{\alpha_1} \alpha_1 + c_3 \alpha_1^2 = 0 \tag{7}$$

$$\ddot{\alpha_1} + \omega_1^2 \alpha_1 + 2\mu_2 \dot{\alpha_1} + 2mc_7 s\ddot{\alpha_1} + 2mc_7 \dot{s}\dot{\alpha_1} + mc_7 \ddot{s}\alpha_1 + c_8 s\alpha_1 = Fcos(\Omega t + \tau) \tag{8}$$

where $Fcos(\Omega t + \tau) = -\phi_1 c_y \ddot{y}$, and μ_n is the normalized damping ratio. Two scales T_0 and T_1 are used:

$$T_0 = t$$

$$T_1 = \varepsilon t$$

where ε is a scaling parameter. The next step is to assume an asymptotic series solution for s and α_1. In this case a two term expansion is assumed:

$$s(t) = \varepsilon s_1(T_0, T_1) + \varepsilon^2 s_2(T_0, T_1) \tag{9}$$

$$\alpha_1(t) = \varepsilon u_1(T_0, T_1) + \varepsilon^2 u_2(T_0, T_1) \tag{10}$$

Where $s_1(T_0, T_1)$ and $s_2(T_0, T_1)$ are the ε^{th} and ε^2 order solutions respectively for the moving mass, and $u_1(T_0, T_1)$ and $u_2(T_0, T_1)$ are the ε^{th} and ε^2 order solutions respectively for the beam. To analyze primary resonances, we arrange the forcing term so that it appears in the same perturbation equation as the nonlinear. To study internal resonance, we consider the case of $\Omega = \omega_1 + \varepsilon\sigma_1$, where σ_1 is a small detuning parameter. We let $F = \varepsilon^2 f$ and $\mu_n = \varepsilon\mu_n$. Substituting (9) and (10) into the governing equation (7) and (8), and setting the coefficients of ε and ε^2 zero gives

ε order:

$$\frac{\partial^2 s_1}{\partial T_0^2} + \omega^2 s_1 = 0 \tag{11}$$

$$\frac{\partial^2 \mathrm{u}_1}{\partial \mathrm{T}_0^2} + \omega_1^2 \mathrm{u}_1 = 0 \tag{12}$$

ε^2order:

$$\frac{\partial^2 s_2}{\partial T_0^2} + \omega^2 s_2 = -2\mu_1 \frac{\partial s_1}{\partial T_0} - 2\frac{\partial^2 s_1}{\partial T_0 \partial T_1} - c\frac{\partial^2 u_1}{\partial T_0^2} u_1 - c_3 u_1^2 \tag{13}$$

$$\frac{\partial^2 u_2}{\partial T_0^2} + \omega_1^2 u_2 = -2\mu_2 \frac{\partial u_1}{\partial T_0} - 2\frac{\partial^2 u_1}{\partial T_0 \partial T_1} - 2mc_7 \frac{\partial^2 u_1}{\partial T_0^2} s_1 - 2mc_7 \frac{\partial s_1}{\partial T_0}\frac{\partial u_1}{\partial T_0} - mc_7 \frac{\partial^2 s_1}{\partial T_0^2} u_1 - c_8 s_1 u_1 + f\cos(\Omega T_0 + \tau) \tag{14}$$

The solution to (11) and (12) are given by:

$$s_1 = P_1(T_1)e^{i\omega T_0} + \overline{P_1}(T_1)e^{-i\omega T_0} \tag{15}$$

$$u_1 = P_2(T_1)e^{i\omega_1 T_0} + \overline{P_2}(T_1)e^{-i\omega_1 T_0} \tag{16}$$

Where P_1 and P_2 a complex variables. The overbars in (15) and (16) denote the complex conjugate. Substituting (15) and (16) into the right hand sides of (13) and (14) results in

$$rhs(13) = -2\mu_1 i\omega P_1 e^{i\omega T_0} + 2\mu_1 i\omega \bar{P}_1 e^{-i\omega T_0} - 2i\omega \frac{\partial P_1}{\partial T_1} e^{i\omega T_0} + 2i\omega \frac{\partial \overline{P_1}}{\partial T_1} e^{-i\omega T_0} + \left(c_1\omega_1^2 P_2 e^{i\omega_1 T_0} + c_1\omega_1^2 \overline{P_2} e^{-i\omega_1 T_0}\right)\left(P_2 e^{i\omega_1 T_0} + \overline{P_2} e^{-i\omega_1 T_0}\right) - c_3 P_2^2 e^{2i\omega_1 T_0} - 2c_3 P_2 \overline{P_2} - c_3 \overline{p_2}^2 e^{-2i\omega_1 T_0} \quad (17)$$

$$rhs(14) = -2\mu_2 i\omega_1 P_2 e^{i\omega T_0} + 2\mu_2 i\omega_1 \bar{P}_2 e^{-i\omega T_0} - 2i \frac{\partial P_2}{\partial T_1} \omega_1 e^{i\omega_1 T_0} + mc_7(2\omega_1^2 + \omega^2 + 2\omega\omega_1) P_1 P_2 e^{i(\omega_1+\omega)T_0} + mc_7(2\omega_1^2 + \omega^2 - 2\omega\omega_1)\overline{P}_1 P_2 e^{i(\omega_1-\omega)T_0} + 2i \frac{\partial \overline{P}_2}{\partial T_1} \omega_1 e^{-i\omega_1 T_0} + mc_7(2\omega_1^2 + \omega^2 + 2\omega\omega_1)\overline{P}_1 \overline{P}_2 e^{-i(\omega_1+\omega)T_0} + mc_7(2\omega_1^2 + \omega^2 - 2\omega\omega_1) P_1 \overline{P}_2 e^{-i(\omega_1-\omega)T_0} - c_8\left(P_1 e^{i\omega T_0} + \overline{P}_1 e^{-i\omega_1 T_0}\right)\left(P_2 e^{i\omega T_0} + \overline{P}_2 e^{-i\omega_1 T_0}\right) + \frac{1}{2} f e^{i\omega_1 T_0} e^{i(\sigma_1 T_1 + \tau)} + \frac{1}{2} f e^{-i\omega_1 T_0} e^{-i(\sigma_1 T_1 + \tau)} \quad (18)$$

To eliminate the secular terms the coefficients of $e^{i\omega T_0}$ and $e^{i\omega_1 T_0}$ are set to zero. To study the coupled dynamic behavior of the system under internal resonance, we assume

$$\omega = 2\omega_1 + \varepsilon\sigma_2 \quad (19)$$

where σ_2 is a small detuning parameter. When σ_2 is zero, we have internal resonance of 1:2 ratio (the ratio of the frequency of the moving magnet to the first frequency of the system). In this case, the elimination of secular terms no longer gives linear solution because when we have internal resonance relationship, we have more terms as

$$-2\mu_1 i\omega P_1 - 2i\omega \frac{\partial P_1}{\partial T_1} + c\omega_1^2 P_2^2 e^{-i\sigma_2 T_1} - c_3 P_2^2 e^{-i\sigma_2 T_1} = 0 \quad (20)$$

$$-2\mu_2 i\omega_1 P_2 - 2i\omega_1 \frac{\partial P_2}{\partial T_1} + (2mc_7\omega_1^2 - 2mc_7\omega_1\omega + mc_7\omega^2 - c_8) P_1 \bar{P}_2 e^{i\sigma_2 T_1} + \frac{1}{2} f e^{i(\sigma_1 T_1 + \tau)} = 0 \quad (21)$$

The complex P_1 and P_2 are described as polar form as

$$P_1(T_1) = \frac{1}{2} p_1(T_1) e^{i\varphi_1(T_1)}$$

$$P_2(T_1) = \frac{1}{2} p_2(T_1) e^{i\varphi_2(T_1)}$$

Set real part and imaginary part of (20) and (21) to zero respectively, to obtain

$$\frac{\partial p_1}{\partial T_1} = -\mu_1 p_1 + \frac{a_{11}}{4\omega} p_2^2 sin\gamma_1 \quad (22)$$

$$p_1 \frac{\partial \varphi_1}{\partial T_1} = -\frac{a_{11}}{4\omega} p_2^2 cos\gamma_1 \quad (23)$$

$$\frac{\partial p_2}{\partial T_1} = -\mu_2 p_2 - a_{22} \frac{p_1 p_2}{4\omega_1} sin\gamma_1 + \frac{f}{2\omega_1} sin\gamma_2 \quad (24)$$

$$p_2 \frac{\partial \varphi_2}{\partial T_1} = -a_{22} \frac{p_1 p_2}{4\omega_1} cos\gamma_1 - \frac{f}{2\omega_1} cos\gamma_2 \quad (25)$$

where

$$a_{11} = c\omega_1^2 - c_3$$

$$a_{22} = 2mc_7\omega_1^2 - 2mc_7\omega_1\omega + mc_7\omega^2 - c_8$$

$$\gamma_1 = 2\varphi_2 - \varphi_1 - \sigma_2 T_1$$

$$\gamma_2 = \sigma_1 T_1 + \tau - \varphi_2$$

In equation (22)-(25), p_1 and p_2 are the modal amplitudes and φ_1 and φ_2 are corresponding phase. For the steady-state response, we set $\frac{\partial p_1}{\partial T_1} = \frac{\partial p_2}{\partial T_1} = \frac{\partial \gamma_1}{\partial T_1} = \frac{\partial \gamma_2}{\partial T_1} = 0$ and solve them numerically. The stability of the steady-state response can be determined via the Lyapunov theory. If all the eigenvalues of Jacobian matrix have negative real parts, the corresponding steady state response is stable. If not, the corresponding steady-state response is unstable.

4 PARAMETERIC STUDY

With the selection of paramters in Table 1, internal resonance of 1:2 occurs at $\omega = 32Hz$ and $\omega_1 = 16Hz$, meaning the detuning parameter $\sigma_2 \approx 0$.

Table 1 Parameters used in simulation of Figure 3

Parameters	Valus
Mass of moving magnet (m)	4g
Mass of beam	5.6g
Length (L)	75mm
Young`s modulus and inertia moment (EI)	$0.003Pa \cdot m^4$
Normalized damping ratio (μ_1 and μ_2)	0.02
Stiffness of the spring (k)	250N/m
Original length of the spring (s_0)	57.75mm
Distance between the tip of beam and magnet (d)	4.5mm
Magnetization moment	0.5 Am^2

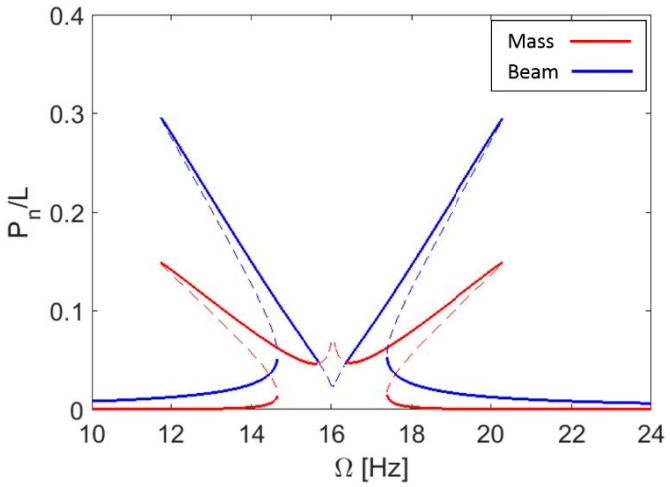

Figure 3 Frequency response for the cantilever and moving magnet.

The default value of base excitation is set to nondimensional value of $f = 0.1$, which corresponds to 1g. The corresponding frequency response is shown in Figure 3 for the beam and the moving magnet. Solide lines represent the

stable responses and dashed lines represent the unstable responses. Jumping phenomenon is observed varying the frequency Ω. There are two branches that are tilted to opposite directions leading to a boradband frequency response. For some combinations of the parameters, there exists a region near the center frequency, where the solution is unstable. Since only the response of the cantilever affects the voltage production of a piezoelectric strip at its base, for the rest of the analysis, only the beam response is illustarted. We study the effect of system parameters on the frequency responses in the subsequent figures.

Figure 4 shows the displacement frequency response curves for different stiffness values of spring. As the k is smaller than 250N/m, the peak of right branch is larger than left peak. The central frequency shifts to the left. The reason is $\omega < 2\omega_1$ that means $\sigma_2 < 0$. It presents a better performance on the right side of central frequecy. On the contrary, when k increases, the curve shifts to the right that is because of $\omega > 2\omega_1$.

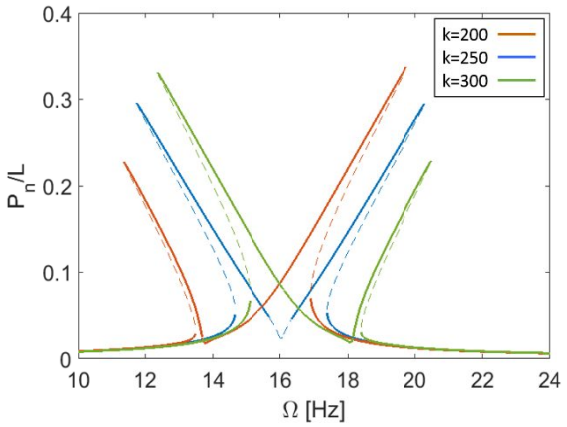

Figure 4 Frequency response for different k (N/m)

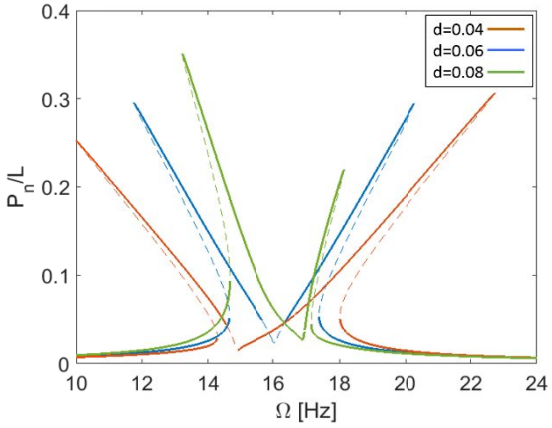

Figure 5 Frequency response for different d (d/L)

Figure 5 depicts the frequency response for different d, the distance between the tip of cantilever to the fixed magnet. Result shows that when d decreases, a broader bandwidth response is obtained with a shift of the central frequency to left. At smaller d values, the magnetic force influences the system more than the case where d is large. Stronger magnetic force creates stronger bi-stability effect, that causes larger tilting in the frequency response while maintaning the same peak amplitude in the response.

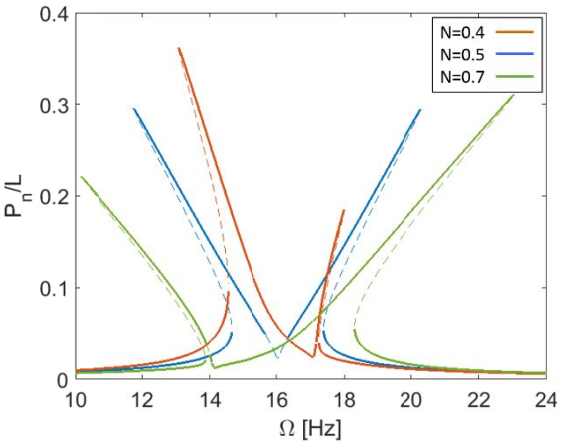

Figure 6 Frequency response for different Magnetization N (Am^2).

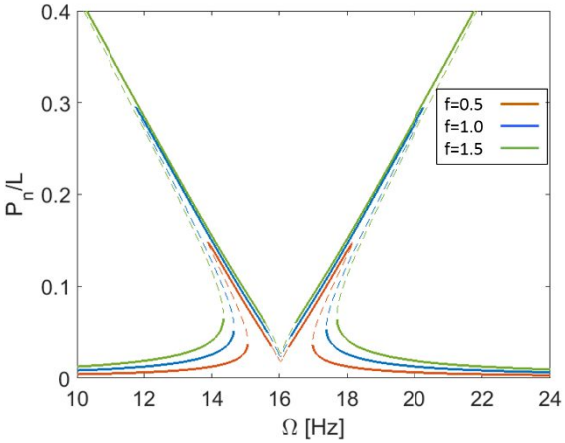

Figure 7 Frequency response for different excitation levels f (g).

Figure 6 plots the frequency response curves for different magnetization moment. It presents similar qualitative results as changing d. In fact, changing the magnetization is analogous to changing of the initial distance of the magnets. With the

larger magnetic force, the system has a broader bandwidth as the effect of bi-stability caused by the magnets, becomes stronger.

Figure 7 shows the displacement frequency response curves for different levels of base excitation. It reveals the effect of the external excitation amplitude on the frequency response curves. It is observed that the unstable solution in the middle increases with increasing the level of excitation. Both the response amplitude and the resonance range increase with the excitation amplitude, but it does not affect the tilting of the frequency response unlike bi-stable resonators with fixed magnets [9].

CONCLUSION

This study explores the behavior of a hybrid resonator that combines internal resonance with bi-stability to increase frequency bandwidth. The hybrid resonator consists of a cantilever beam carrying a moving magnet attached to a spring and a fixed magnet. The presence of two magnets creates a bi-stable system, while making one magnet movable using a spring adds internal resonance. The governing equations are obtained using Hamilton's energy approach for the first mode shape of the beam. The perturbation method of multiple scales is employed to obtain the frequency responses. The frequency response results reveal a double bending effect, two frequency peaks bending to opposite sides, resulting in a broader frequency bandwidth. The effects of different system parameters are studied on the frequency response curves. It is concluded that larger magnetic forces, softer springs, and smaller initial distances between magnets foster the bi-stable behavior effect and cause larger tilting in the frequency response (broader frequency bandwidth). It is noted that a broad bandwidth is obtained, while the peak amplitude is maintained. This study provides a platform to design a hybrid resonator with increased frequency bandwidth to improve energy conversion efficiency in vibration energy harvesters.

REFERENCES

[1] Cottone F., Vocca H. and Gammaitoni L., "Nonlinear Energy Harvesting," PRL 102, 080601 (2009).
[2] Barton D. A. W., Burrow S. G. and Clare L. R., "Energy Harvesting From Vibrations with a Nonlinear Oscillator," ASME Journal of Vibration and Acoustics, 132: 0210091 (2010).
[3] Mann B. P. and Owens B. A., "Investigations of a nonlinear energy harvester with a bistable potential well", Journal of Sound and Vibration, 329(9):1215–1226 (2010).
[4] Mann B. P. and Sims N. D., "Energy harvesting from the nonlinear oscillations of magnetic levitation", Journal of Sound and Vibration, 319(1-2):515–530 (2009).
[5] Tang L., Yang Y. and Soh C. K., "Toward Broadband Vibration-based Energy Harvesting", Journal of Intelligent Material Systems and Structures, 21(18):1867–1897 (2010).
[6] Vocca H., Neri I., Travasso F. and Gammaitoni L., "Kinetic energy harvesting with bistable oscillators", Applied Energy, 97:771–776 (2012).
[7] Ando B., Baglio S., Maiorca F. and Trigona C., "Analysis of two dimensional, wide-band, bistable vibration energy harvester", Sensors and Actuators A: Physical, 202:176–182 (2013).
[8] Masana R. and Daqaq M. F., "Relative performance of a vibratory energy harvester in monoand bi-stable potentials", Journal of Sound and Vibration, 330(24):6036–6052 (2011).
[9] Stanton S. C., McGehee C. C and Mann B. P., "Nonlinear dynamics for broadband energy harvesting: Investigation of a bistable piezoelectric inertial generator," Physica D 239 640-653 (2010).
[10] Ferrari M., Ferrari V., Guizzetti M., Ando B., Baglio S. and Trigona C., "Improved energy harvesting from wideband vibrations by nonlinear piezoelectric converters," Sensors and Actuators A 162 425-431 (2010).
[11] Daqaq. M. F.,"Response of uni-modal duffing-type harvesters to random forced excitations," Journal of Sound and Vibration, 329(18):3621–3631 (2010).
[12] Ando B., Baglio S., Trigona C., Dumas N., Latorre L. and Nouet P., "Nonlinear mechanism in MEMS devices for energy harvesting applications", J. Micromecha. Microeng. 20 125020, (12pp) (2010).
[13] Nayfeh A. H. and Mook, D. T., [Nonlinear oscillations], Wiley, New York (1979).
[14] Chen L. Q., "Internal resonance energy harvesting," Journal of Applied Mechanics, 031004-1 (2015).

[15] Siddiqui S. A. Q., Golnaraghi M. F. and Heppler G. R., “Dynamics of a flexible cantilever beam carrying a moving mass,” Nonlinear Dynamics 15:137-154 (1998).
[16] Jia Y. and Seshia A. A., “An auto-parametrically excited vibration energy harvester,” Sensor and Actuators, A 220 69-75 (2014).
[17] Jia Y., Yan J., Soga K. and Seshia A. A., “Parametrically excited mems vibrations energy harvesters.” PowerMEMS (2012).